

## NEW OBSERVATIONAL CONSTRAINTS ON THE GROWTH OF THE FIRST SUPERMASSIVE BLACK HOLES

E. TREISTER<sup>1</sup>, K. SCHAWINSKI<sup>2</sup>, M. VOLONTERI<sup>3</sup> AND P. NATARAJAN<sup>4,5,6</sup>  
*ApJ, Accepted*

### ABSTRACT

We constrain the total accreted mass density in supermassive black holes at  $z > 6$ , inferred via the upper limit derived from the integrated X-ray emission from a sample of photometrically selected galaxy candidates. Studying galaxies obtained from the deepest Hubble Space Telescope images combined with the *Chandra* 4 Msec observations of the *Chandra* Deep Field South, we achieve the most restrictive constraints on total black hole growth in the early Universe. We estimate an accreted mass density  $< 1000 M_{\odot} \text{Mpc}^{-3}$  at  $z \sim 6$ , significantly lower than the previous predictions from some existing models of early black hole growth and earlier prior observations. These results place interesting constraints on early black growth and mass assembly by accretion and imply one or more of the following: (1) only a fraction of the luminous galaxies at this epoch contain active black holes; (2) most black hole growth at early epochs happens in dusty and/or less massive - as yet undetected - host galaxies; (3) there is a significant fraction of low- $z$  interlopers in the galaxy sample; (4) early black hole growth is radiatively inefficient, heavily obscured and/or is due to black hole mergers as opposed to accretion or (5) the bulk of the black hole growth occurs at late times. All of these possibilities have important implications for our understanding of high redshift seed formation models.

*Subject headings:* galaxies: active — galaxies: Seyfert — X-rays: galaxies

### 1. INTRODUCTION

One of the most challenging problems in astronomy today is understanding how and when the first supermassive black holes (SMBHs) in the Universe formed. It is widely believed that most of their growth happens primarily via accretion episodes (Soltan 1982). The detection of luminous quasars at the earliest epochs implies that the rare behemoths with masses in excess of  $10^8 M_{\odot}$  are already in place by  $z \sim 7$ . The nature of the galaxies that host these is as yet unsettled due to the limitations of current observational technologies. Recently, it has been possible to detect the brightest most copiously star forming galaxies at these epochs via the photometric drop-out technique. A natural question is if these are the brightest and therefore the most massive galaxies at these epochs, then do they host the most massive black holes as the local demography of black holes suggests? We are now in a position to examine this issue with adequate data combining sources selected as part of the Hubble Ultra Deep Field (HUDF) and the Cosmic Assembly Near-IR Deep Extragalactic Legacy Survey (CANDELS).

Nevertheless, deeply interconnected with this question are those of how the first black hole (BH) seeds form and when. Several possibilities for the formation of

these seeds have been hypothesized (see Volonteri 2010; Natarajan 2011, for reviews), however two remain the most accepted modes. The first one postulates that BH seeds result from the remnants of the first stars, the so-called population III generation stars (e.g., Abel et al. 2000; Madau & Rees 2001; Bromm et al. 2002). Simulations suggest that these stars form from the collapse of primordial, metal-free, gas clouds at  $z \sim 20$ , and have masses greater than  $30 M_{\odot}$  (Tan & McKee 2004), implying very short lifetimes (Abel et al. 2002). Upon rapid exhaustion of fuel, these stars likely lead to the formation of seed BHs with masses  $\sim 10$ - $100 M_{\odot}$  depending on the initial masses of the Pop III stars. The second possibility is a heuristic picture wherein early black hole seeds could form via direct gravitational collapse of gas-rich pre-galactic disks, leading to significantly more massive seed masses with  $M_{\text{seeds}} \sim 10^5 M_{\odot}$  (Loeb & Rasio 1994; Bromm & Loeb 2003; Begelman et al. 2006; Lodato & Natarajan 2006).

Recent observations suggest that massive, a few  $M \sim 10^9 M_{\odot}$ , BHs were already in place by  $z \sim 7$  (e.g., Mortlock et al. 2011), i.e.,  $\sim 800$  million years after the Big Bang. While these early massive BHs, which are detected as high-luminosity quasars, are very rare (Fan et al. 2004; Willott et al. 2010b), they do suggest that some fraction of BH seeds likely grow rapidly in the early Universe. These extreme sources, due to their extraordinary growth history, while individually interesting, have limited utility for probing the first BH growth episodes for the population as a whole. In fact, it is the lower mass, more common BHs, representative of the average population that are needed to constrain early growth and seed assembly scenarios. Directly examining such low mass – and therefore low-luminosity – BHs at  $z \geq 6$  is impossible with current observational instruments. The best we can do at the present time is therefore to stack

<sup>1</sup> Universidad de Concepción, Departamento de Astronomía, Casilla 160-C, Concepción, Chile; etreiste@astro-udec.cl

<sup>2</sup> Institute for Astronomy, Department of Physics, ETH Zurich, Wolfgang-Pauli-Strasse 16, CH-8093 Zurich, Switzerland

<sup>3</sup> Institut d'Astrophysique de Paris, 98bis Bd. Arago, 75014 Paris, France

<sup>4</sup> Yale Center for Astronomy and Astrophysics, P.O. Box 208121, New Haven, CT 06520.

<sup>5</sup> Department of Physics, Yale University, P.O. Box 208121, New Haven, CT 06520.

<sup>6</sup> Department of Astronomy, Yale University, PO Box 208101, New Haven, CT 06520.

data as the only way to access the earliest phases of black hole growth and discern the average properties of the population.

Observations at X-ray wavelengths are most suitable method for tracing BH growth as hard X-ray emission is the most reliable signpost for accretion. In this work, we study the X-ray properties of a sample of galaxies at  $z=6-8$  selected based on the deepest observed-frame optical and near-IR images obtained with the Hubble Space Telescope (HST) to date from the HUDF and the CANDELS survey. We take advantage of the 4 Msec Chandra observations of the Chandra Deep Field South (CDF-S) — the deepest X-ray observation ever taken — in order to constrain the integrated accreted BH mass density at  $z>6$  and compare with existing models of BH formation and early growth. Throughout this letter, we assume a  $\Lambda$ CDM cosmology with  $h_0=0.7$ ,  $\Omega_m=0.27$  and  $\Omega_\Lambda=0.73$  (Hinshaw et al. 2009).

## 2. OBSERVATIONAL RESULTS

Thanks to the 4 Msec Chandra observations (Xue et al. 2011), the CDF-S is the field with the deepest currently-available X-ray observations. Our target sample of high- $z$  galaxy candidates was constructed using a combination of Lyman Break Galaxies (LBGs), selected using the optical and near-IR selection techniques described by e.g., Bouwens et al. (2006, hereafter B06), and galaxies at  $z>6$  based on their photometric redshifts obtained by performing spectral fitting. Using the deep HST observations available in this field, B06 reported the finding of 371  $z\sim 6$  galaxy candidates, while later observations obtained using the WFC3 camera allowed for the detection of 66 at  $z\sim 7$  and 47 at  $z\sim 8$  (Bouwens et al. 2011, B11 hereafter). More recently, Finkelstein et al. (2012, hereafter F12), using the HST/WFC3 observations of the CANDELS fields obtained a sample of 223 galaxies at  $z\sim 6$ , 80 at  $z\sim 7$  and 33 at  $z\sim 8$ , all of them selected via photometric redshifts. The combination of these sources constitute the main sample for this work.

As can be seen in Fig. 1, the sources are not evenly distributed in the sky. The density is higher in the HUDF field, which is expected given the deeper optical and near-IR observations available there. On average, sources in the HUDF are  $\sim 3'$  away from the Chandra pointing center. The solid area covered by the  $z\sim 6$  B06 sample is  $\sim 160$  arcmin<sup>2</sup>, i.e. the GOODS-S region, which is almost completely included in the Chandra  $8'$  radius. At  $z\sim 7$  and  $z\sim 8$  sources are strongly clustered in the  $\sim 5$  arcmin<sup>2</sup> field. In the case of the F12 sample, sources are spread more evenly across the field, while a higher density is still observed in the HUDF region, due to the deeper data available there.

None of these high- $z$  candidates is detected individually in X-rays (using a  $2''$  search radius). Figures 2 and 3 show the effective X-ray counts of each source — further details can be found in Treister et al. (2011) and Cowie et al. (2012) — for the sources in the B06, F12 and the combined samples. The X-ray properties of the sources at  $z\sim 7$  and  $z\sim 8$  in the B11 sample, not shown in these figures, are similar to those in the F12 sample at those redshifts. As can be clearly seen, no individual source is detected beyond the  $\sim 3\text{-}\sigma$  level in either the observed-frame soft (0.5-2 keV) or hard (2-8 keV) Chandra bands. Therefore, we aim to detect X-ray emission

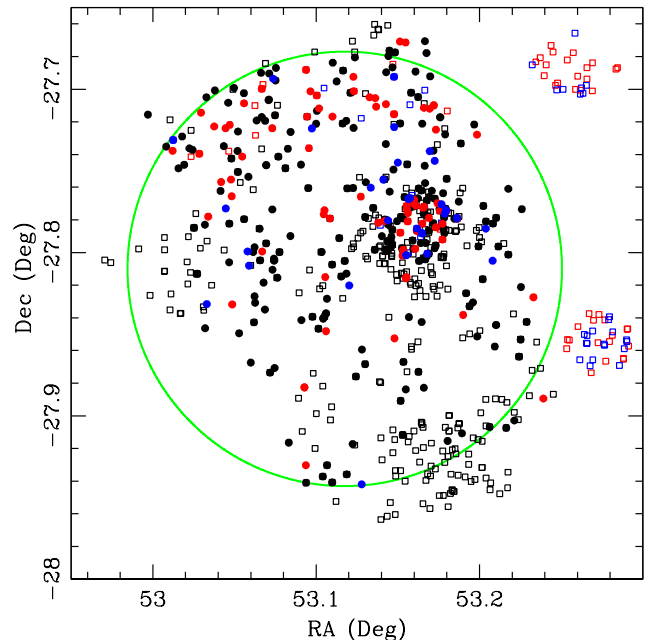


FIG. 1.— Position in the sky of the sources considered in our work. Filled circles show the galaxy candidates from the sample of F12, while the squares present the LBGs from the work of B06 ( $z\sim 6$ ) and B11 ( $z\sim 7$  and  $z\sim 8$ ). Sources at  $z\sim 6$  are shown in black, in red the sources at  $z\sim 7$  and in blue at  $z\sim 8$ . The field is centered in the aim point of the Chandra CDF-S observations, while the green line shows a  $8'$  radius circle. Sources inside this circle were considered for X-ray stacking. The two groups clearly visible outside the green circle correspond to the Hubble parallel fields.

from these sources using stacking. Specifically, we followed the procedure of Treister et al. (2011), modified to improve the background subtraction as described in Cowie et al. (2012). The main goal of this procedure is to optimize the resulting signal-to-noise ratio (SNR), by introducing a variable aperture size as a function of the off-axis angle relative to the Chandra aimpoint.

In order to maximize the SNR and avoid biasing our estimations of the local background we only considered sources closer than  $8'$  from the Chandra aimpoint ( $03^{\text{h}}32^{\text{m}}28^{\text{s}}06, -27^{\circ}48'26''.4$ ; Xue et al. 2011) that do not have a detected X-ray source at  $<15''$ . With these constraints, we stacked 223, 16 and 11 sources at  $z\sim 6$ ,  $z\sim 7$  and  $z\sim 8$  from the B06 and B11 samples respectively and 137, 40 and 20 sources from the sample of F12. Our results are presented in Table 1. As can be seen, there is no significant detection in any of the samples, thus contradicting the earlier results claimed by Treister et al. (2011). This confirms that, as presented by Willott (2011) and Cowie et al. (2012), the results in Treister et al. (2011) likely arise from their background subtraction technique.

As shown in Figure 1, given that the depth of the optical and near-IR coverage of the field studied here is not homogeneous, and that we did not obtain a significant detection by stacking the entire sample of galaxies at  $z\sim 6$ ,  $z\sim 7$  and  $z\sim 8$ , we attempted to stack the most luminous optical/near-IR galaxies, which can be detected

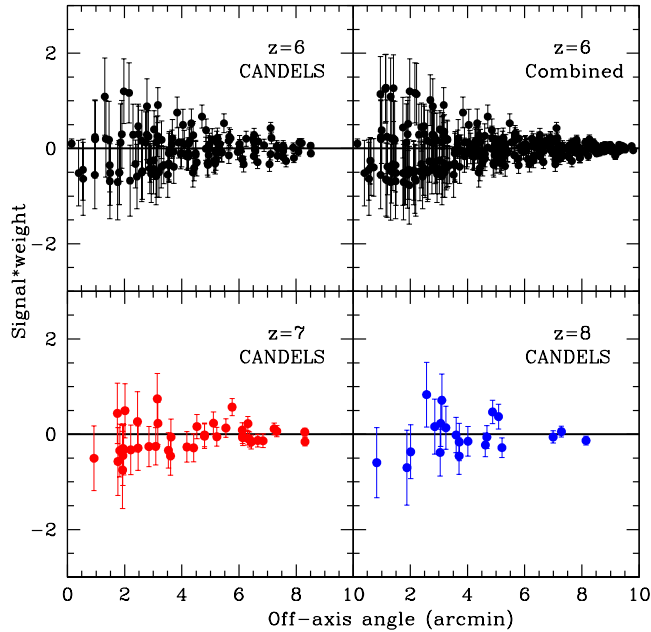


FIG. 2.— Effective background-subtracted signal in the soft X-ray (0.5-2 keV) band measured using the procedure described by Treister et al. (2011) and the background subtraction algorithm of Cowie et al. (2012) for the sources in the F12 and the combined samples as a function of off-axis angle. The observed background-subtracted counts are weighted to account for the differences in exposure time, aperture corrections and sensitivity, as described by Treister et al. (2011). Clearly, no source is individually detected beyond the  $3\text{-}\sigma$  level. Furthermore, the total signal is consistent with zero, thus confirming that no detection in the stacked samples is found either.

across the whole field. Specifically, we performed independent stacks for different cuts in optical and near-IR fluxes. None of these stacks yielded a significant detection either.

To establish the statistical significance of the non-detections in the entire sample and translate them into upper limits on the stacked X-ray emission we perform independent Monte Carlo simulations for each of these samples. This is done by computing the obtained SNR in 500 stacks, in which the position of each stacked source was shifted randomly in right ascension and declination in the  $5''\text{-}15''$  range. For both bands, the resulting distributions are well fitted by Gaussian functions with mean  $\simeq 0$  and standard deviation  $\simeq 1$ , as expected. The SNR distributions obtained in our Monte Carlo simulations is shown in Figure 4.

We then compute  $3\sigma$  upper limits for the X-ray emission from these samples. Focusing solely on the joint samples, in order to maximize the number of sources, we find for the  $z\sim 6$  sources an upper limit for the X-ray luminosity of  $2.6\times 10^{41}$  erg  $\text{s}^{-1}$  in the soft band,  $\sim 2\times$  smaller than the upper limit reported by Cowie et al. (2012). This is as expected due to the increased sample size providing a tighter upper limit. In the hard band, we compute an upper limit of  $1.6\times 10^{42}$  erg  $\text{s}^{-1}$ . Similarly, for the  $z\sim 7$  galaxies the upper limits are  $6.8\times 10^{41}$  erg  $\text{s}^{-1}$  and  $5.3\times 10^{42}$  erg  $\text{s}^{-1}$  in the soft and hard bands re-

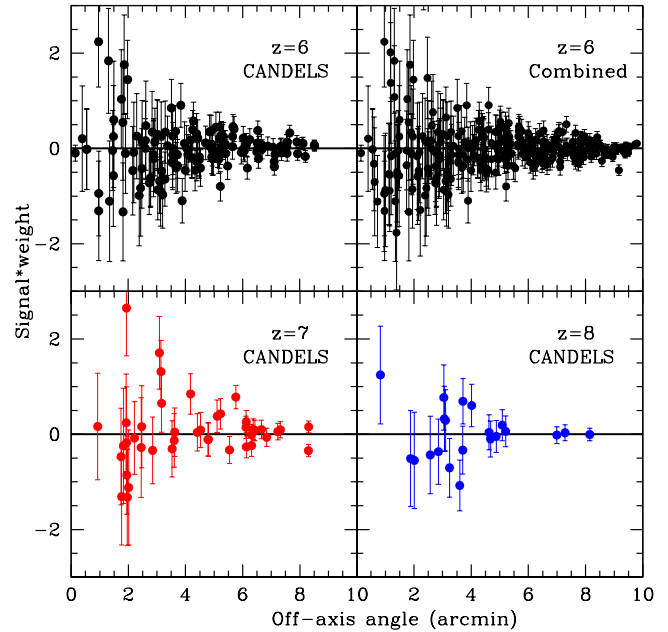


FIG. 3.— Effective background-subtracted counts in the hard X-ray (2-8 keV) band measured using the procedure described by Treister et al. (2011) and the background subtraction algorithm of Cowie et al. (2012) for the sources in the F12 and the combined samples as a function of off-axis angle. Symbols are the same as in Fig. 2. As in the previous case, no source is individually detected in this band beyond the  $3\text{-}\sigma$  level.

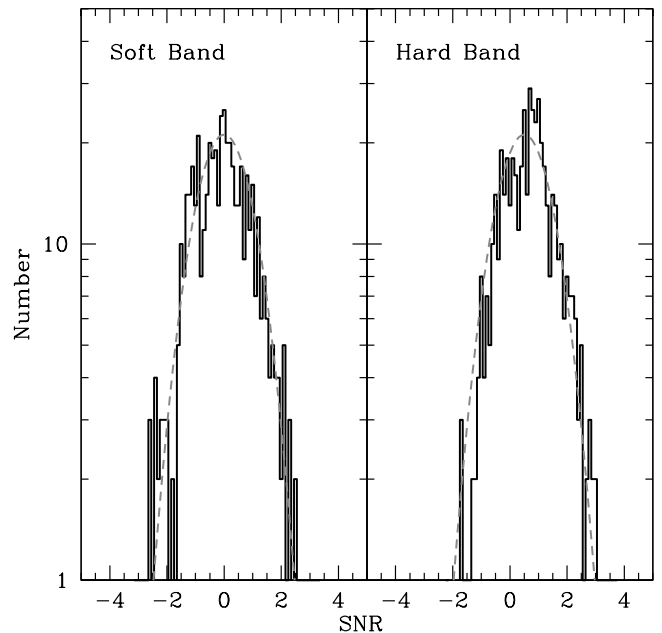


FIG. 4.— Distribution of SNR obtained for 500 independent stacks, in which the position of each stacked source was shifted randomly in the soft (left panel) and hard (right panel) Chandra bands. The gray dashed lines in each panel show the best-fitting gaussian fits, with mean  $\simeq 0$  (0.5 for the hard band) and standard deviation  $\simeq 1$ .

spectively. At  $z\sim 8$ , these are  $1.5\times 10^{42}$  erg  $s^{-1}$  and  $9.8\times 10^{42}$  erg  $s^{-1}$ .

Similar measurements were performed recently by Fiore et al. (2012) and Basu-Zych et al. (2013) among others, finding consistent results. For example, Basu-Zych et al. (2013) report upper limits in the rest-frame 2-10 keV band of  $4.2\times 10^{41}$  erg  $s^{-1}$  at  $z\sim 6$ ,  $9.5\times 10^{41}$  erg  $s^{-1}$  at  $z\sim 7$  and  $1.6\times 10^{42}$  erg  $s^{-1}$  at  $z\sim 8$ . These are slightly higher but fully consistent with the upper limits for the stacked X-ray luminosities reported here. The (small) differences can be due to the stacking technique used and the minor differences between the galaxy samples.

It is important to note that both the samples of B06 and F12 explicitly exclude point-like (spatially unresolved) sources. Most of the high- $z$  galaxy candidates are spatially resolved, and so only a small fraction of sources ( $\sim 5\%$ ) are removed by this requirement. While this is done to reduce the stellar contamination, it could represent a bias against unobscured Active Galactic Nuclei (AGN) in which the nuclear emission dominates the optical light. In order to test for the possible effects of this criterion, we independently stack the sample of 11 point-like  $i$ -dropouts in the HDF-S reported by Bouwens et al. (2006), in their Table 3. Consistent with the results obtained from the resolved sample, we do not find a significant detection in X-ray stacking in neither the soft nor the hard *Chandra* bands. Therefore, we conclude that the exclusion of point-like sources from our main samples does not affect the results reported here.

### 3. DISCUSSION

With the upper limits obtained above, we can derive the most stringent observational constraints to date on the early growth of the first SMBHs. We first note that the upper limits obtained here are lower than the standard threshold for AGN-dominated X-ray emission (e.g. Szokoly et al. 2004),  $\sim 10^{42}$  erg  $s^{-1}$ . Therefore, we can conclude that **either no luminous AGN are present in any of the samples studied here or the occupation fraction of such AGN is so low that the signal gets diluted in the stacking procedure.**

If we proceed under the assumption that the luminosity of these sources derives entirely from star formation (i.e. no AGN are present), as proposed previously by Cowie et al. (2012), these upper limits can then in turn be used as an observational constraint on the average star formation rate (SFR). Taking into account the tight correlation between X-ray luminosity and SFR in absence of AGN emission measured by Ranalli et al. (2003) and more recently by Lehmer et al. (2010), we can compute an upper limit for the average SFR in these samples. Since these are relatively low-mass galaxies, with typical stellar masses  $< 10^{10}M_{\odot}$  (González et al. 2011), we can safely neglect the contribution of low mass X-ray binaries to the total X-ray luminosity. Therefore, we can assume that the X-ray luminosity is proportional to the star formation rate (SFR), with a relation given by  $L_{HX} = \beta$  SFR, where  $L_{HX}$  is the rest-frame 2-10 keV luminosity, and  $\beta = 1.62\times 10^{39}$  erg  $s^{-1} (M_{\odot} \text{yr}^{-1})^{-1}$  (Lehmer et al. 2010). While this was established from observations of  $z\sim 0$  galaxies, no evolution in this correlation has been observed up to  $z\sim 1.3$  (Mineo et al. 2012). Assuming that we can extrapolate this relation to  $z\sim 6$  enables the translation of the upper limits of the X-ray luminosity ob-

tained above to SFRs of  $> 210 M_{\odot} \text{yr}^{-1}$  for the  $z\sim 6$  samples,  $> 460 M_{\odot} \text{yr}^{-1}$  at  $z\sim 7$  and  $> 1000 M_{\odot} \text{yr}^{-1}$  at  $z\sim 8$ . In comparison, these upper limits on the SFRs are significantly higher, by an order of magnitude or more, than the estimated values for the SFR reported by González et al. (2010); Curtis-Lake et al. (2013) of  $\sim 5\text{-}20 M_{\odot} \text{yr}^{-1}$  for individual galaxies at these redshifts.

#### 3.1. Accreted Black Hole Mass Density

From the stacked upper limits to the X-ray luminosity we can derive the accreted black hole mass density in these galaxies. In order to do this we follow the procedure outlined in the supplementary information section presented by Treister et al. (2011). Briefly, we base our calculation on the so-called ‘‘Soltan argument’’ (Soltan 1982), from which we have that the integrated black hole mass density is given by:

$$\rho_{BH}(z) = \int_z^{\infty} \frac{dt}{dz} dz \int_0^{\infty} \frac{1-\epsilon}{\epsilon c^2} L_{bol} \Psi(L, z) dL, \quad (1)$$

where

$$L_{bol} = k_{corr} L_X \quad (2)$$

and  $k_{corr}$  is the bolometric correction for the rest-frame hard X-ray band. For simplicity, following Treister et al. (2011), we assume that  $k_{corr}=25$  independent of luminosity and redshift. Then, assuming that the AGN luminosity function does not evolve significantly at  $z>6$  we obtain that:

$$\rho_{BH}(z) = \frac{(1-\epsilon)k_{corr}}{\epsilon c^2} \int_z^{\infty} \frac{dt}{dz} dz \int_0^{\infty} L_X \Psi(L) dL. \quad (3)$$

Here, the second integral on the right side can be determined directly from the observed integrated AGN emissivity. Further assuming a constant radiation efficiency  $\epsilon=0.1$  we obtain the upper limits for the accreted black hole mass density at  $z\sim 6, 7$  and  $8$  reported in Table 1. In comparison, following the same procedure but using the upper limits in the rest-frame hard band and number of sources reported by Basu-Zych et al. (2013), we obtain BH mass densities of 990, 1142 and 1263  $M_{\odot} \text{Mpc}^{-3}$  at  $z\sim 6, 7$  and  $8$  respectively. These values are slightly higher but fully consistent with our results.

In Fig. 5 we show the density of accreted mass onto SMBHs as a function of redshift. In addition to our upper limits at  $6 < z < 8$ , we include the constraints derived by Salvaterra et al. (2012) using the unresolved fraction of the cosmic X-ray background (CXRB), which are less restrictive than our upper limits. However, in contrast to our work, they are independent of the completeness of the galaxy sample studied and correspond to an integral constraint. But, as discussed in Salvaterra et al. (2012), they are affected by degeneracies in the assumed CXRB model, in particular with low-luminosity sources at lower redshifts. Furthermore, as argued by Treister et al. (2009a), the uncertainty in the measurements of the CXRB and discrepancies between those derived by different missions can be  $\sim 10\%$  of the total value, which is orders of magnitude larger than the signal expected to be measured.

In Figure 5 we compare these upper limits with the predictions from the models of Volonteri (2010). In

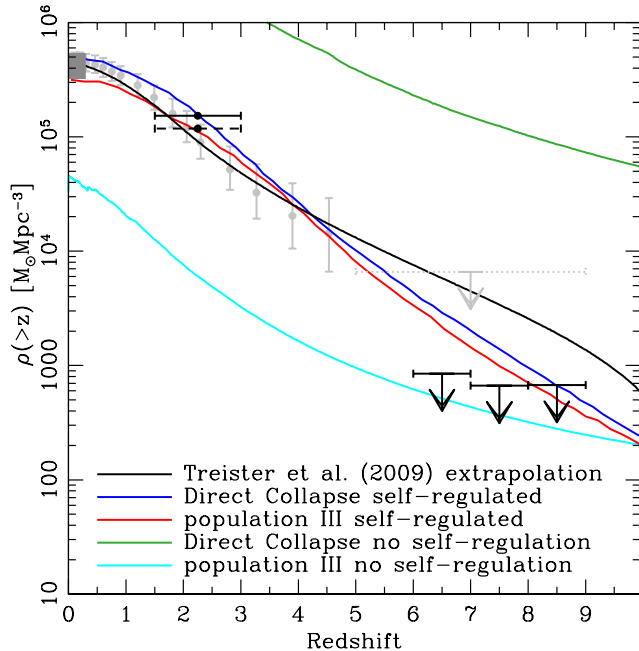


FIG. 5.— Accreted BH mass density as a function of redshift. The gray rectangle shows the range of values allowed by observations of  $z \approx 0$  galaxies (Shankar et al. 2009), while the filled circles show the observations of BH accreted mass density traced by AGN activity in the  $0 < z < 5$  range compiled by Hopkins et al. (2007) and measured by Treister et al. (2009b) at  $z \sim 2$ . At higher redshifts, we show the CXRB integral constraint derived by Salvaterra et al. (2012, upper limit with dotted error bars) and the upper limits at  $z = 6-9$  obtained in this work. The red and blue lines show the predicted BH mass density if self-regulation, as described in section 3.2, is incorporated, for Pop III and direct collapse BH seeds respectively. The cyan and green lines show the results from these models if no regulation is assumed.

these models, two “seed” formation models are considered: those deriving from population-III star remnants (Pop III), and from direct collapse models (D.C.). Independent of the seed mass, in this scheme black holes grow primarily via accretion episodes triggered by galaxy mergers. This growth can be either self-regulated or un-regulated. Details of the implementation of this self-regulation can be found in the supplementary section of Treister et al. (2011). In a nutshell, in the self-regulated model, each black hole accretes an amount of mass, corresponding to 90% of the mass predicted by the local  $M_{\text{BH}} - \sigma$  relation (Gültekin et al. 2009), while in the un-regulated mode the mass is simply doubled during each accretion episode. For this set of models, the only one that satisfies the  $z > 6$  upper limits assumes light black hole seeds (Pop III) and no self-regulation. However, this model fails to account for the observed BH mass density at lower redshifts.

Other models, (e.g., Booth & Schaye 2009; Dubois et al. 2012) predict a much steeper decline in BH mass density at high redshifts and thus are consistent with our observed upper limits. As an example, in Fig. 6, we compare our observational results with the predictions from the models of Bonoli et al. (2012), which incorporate both light (Pop III) and massive (direct collapse) BH seeds. These models assume that a massive, direct col-

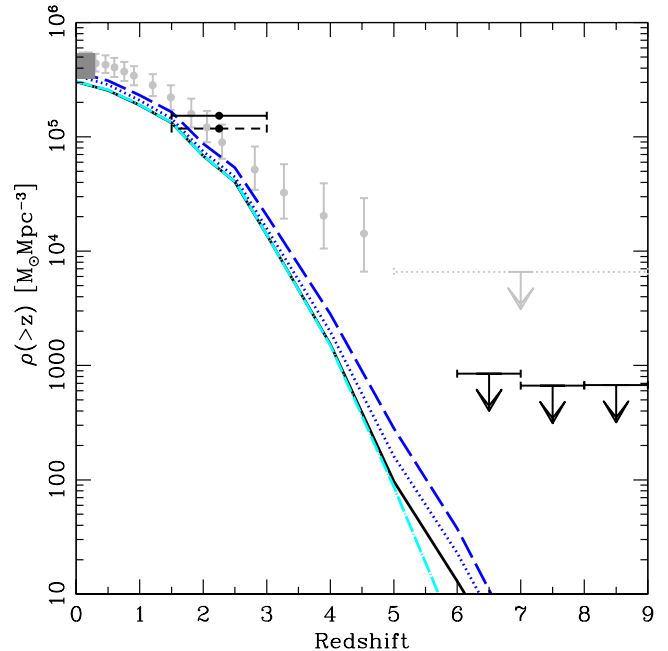


FIG. 6.— Accreted BH mass density as a function of redshift, comparing with the models of Bonoli et al. (2012). Symbols for the observational data are the same as in Fig. 5. The dot-dashed cyan line only considers light (Pop III) BH seeds, while the solid black line and the blue dotted line include both Pop III and direct collapse seeds. The dashed blue line also considers both seed types, but in this case massive seeds can also form in 1:10 mergers. For these models, marginal agreement with observations is obtained at  $z < 3$ , while they are at the same time consistent with our upper limits at  $z > 6$ .

lapse, seed form whenever there is a major merger ( $< 1:3$  mass ratio) of massive galaxies which do not already contain a massive BH, as suggested by (Mayer et al. 2010), although this scenario was later questioned by Ferrara et al. (2013). Further BH growth is then triggered by both major and minor mergers. The main differences between the models compared here to observations, which can explain the differences in BH mass density at high redshift, are the formation epoch of black hole seeds that extends up to nearly  $z \sim 0$  in the Bonoli et al. (2012) models, the assumed average accretion rate, linked to the triggering methods, and their redshift dependence. As can be seen in Fig. 6, while these models are consistent with our observed upper limits at  $z > 6$ , they are only marginally consistent with lower redshift constraints. Furthermore, it is important to note that these models do not include BH growth by secular processes, which can represent a significant fraction of the total BH accretion (Treister et al. 2012; Bellovary et al. 2013), and that the strong decrease in mass density at high redshifts can be due to the limited resolution of the simulations. In summary, we can conclude that spanning the whole range of BH growth, from the most luminous quasars which require massive BHs and very high near-Eddington accretion rates, to our upper limits at  $z > 6$ , which suggest accretion levels lower than  $\sim 10\%$  Eddington, is very difficult to track in simulations and requires strong redshift evolution in most scaling relations (Volonteri & Stark 2011).



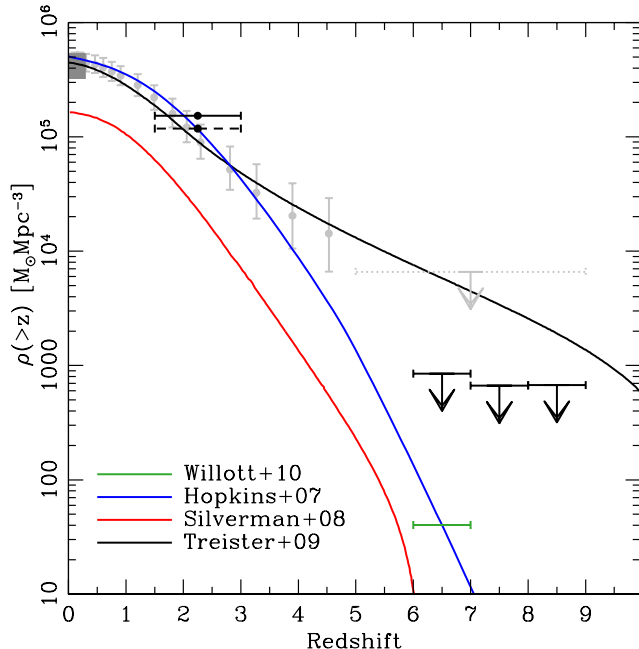


FIG. 7.— Comparison between the observed accreted mass density in SMBHs and expectations from AGN LFs. Observed symbols are the same as in Fig. 5. The *red* and *blue* lines show the values inferred from the LFs of Silverman et al. (2008) and Hopkins et al. (2007) respectively, while the point at  $z=6-7$  was obtained from the quasar LF of Willott et al. (2010b). The *black line* assumes the hard X-ray AGN LF of Ueda et al. (2003), as modified by Treister et al. (2009a).

Comparing with extrapolations of AGN LFs, as shown in Figure 7, the value reported by Willott et al. (2010b) — based on observations of high- $z$  optical quasars — is consistent with the upper limits derived here. Similarly, the bolometric luminosity function of Hopkins et al. (2007) provides a good description of the observed accreted BH mass density at  $z < 4$  and is consistent with our upper limits. In contrast, while the prediction of Treister et al. (2009a), based on an extrapolation of the Ueda et al. (2003) AGN LF, provides the best description of the observational data up to  $z \sim 5$  is clearly inconsistent with the  $6 < z < 9$  upper limits derived in this work, and in marginal agreement with the constraints of Salvaterra et al. (2012).

It is important to note that the tension between the upper limits reported here and at least some of the extrapolations of the AGN LF to high redshifts can be alleviated if uncertainties in the former are considered. For example, a constant radiation efficiency was assumed, while it is possible that most of the BH growth is radiatively inefficient. Similarly, if most of the black hole growth at high redshift is heavily obscured, it would change our assumed bolometric corrections, thus moving the reported upper limits towards higher accreted black hole mass densities. These effects and others are discussed in more detail in the following section.

### 3.2. Where are the Growing Black Holes?

Our observations thus pose a puzzle: the X-ray stack of a sample of star-forming high-redshift dropout galax-

ies shows rather feeble if no signs of BH accretion, despite a favorable environment for accretion - a gas-rich galaxy. We now reflect on what this means both in the context of existing models (e.g., Volonteri 2010) and extrapolations of the AGN LF (e.g., Treister et al. 2009a). We discuss a number of possible explanations, which are neither exhaustive nor mutually exclusive. We note there is a crucial distinction between occupation fraction for SMBHs and AGN fraction. The occupation fraction is a measure of whether a galaxy or halo is seeded with a BH regardless of whether it is actively accreting. If it is actively accreting, it is classified as an AGN and contributes to the estimate of the AGN fraction. For example, even with a high occupation fraction, it is possible that only in a small subset of the galaxies studied here the BH is actively accreting and growing, thus revealing itself as an AGN.

The first possibility to consider is that the galaxies included in our samples do not contain SMBHs or only a small fraction of them do. If this is the case, this is telling us about the efficiency of seed formation. Indeed, as described by e.g., Menou et al. (2001), it is theoretically possible and permissible that at high redshifts only a small fraction of the galaxies actually harbor a SMBH. For example, Menou et al. (2001) showed that with a BH occupation fraction as low as  $\sim 10\%$  at  $z=5$  there are ample seeds for all the galaxies in the local Universe to harbor a central SMBH. This is explained by the sequence of mergers that dark matter halos will experience across cosmic history that will populate black holes into galactic nuclei that are initially bereft of them. What fraction of occupied galaxies host actively accreting ones is a further question. If indeed less than  $\sim 1$  in 10 of the galaxies studied here actually contain a SMBH and perhaps only a fraction of them are actively growing, our X-ray stacking procedure will not be sensitive enough to detect them. This could clearly explain and account for our observational results.

However, it is possible that our sample of LBGs contain SMBHs, but they are not actually growing. Indeed, at lower redshifts,  $z \sim 3$ , the fraction of AGN in Lyman break galaxies is relatively low,  $\sim 3\%$  (Nandra et al. 2002; Laird et al. 2006; Hainline et al. 2012). Likewise, in the recent study of Cowie et al. (2012), samples of Lyman break galaxies at  $z \sim 3, 4$  and 5 were not detected in sensitive X-ray stacks, thus suggesting a low AGN fraction for our sample of LBGs at  $z > 6$  if this trend were to hold at higher redshifts as well. Therefore, while the occupation fraction might be high, the AGN fraction appears to be very low for this sample.

As a caveat, there are significant differences between those lower redshift samples and the  $z > 6$  Lyman break galaxies studied in our work here. For example, high redshift LBGs have significantly lower stellar masses and similar or higher star formation rates (by no more than a factor of two difference between  $z \sim 3$  and  $z \sim 4$ ) (Verma et al. 2007) and (Reddy et al. 2012), and thus much higher sSFRs, indicative of higher gas fractions. In recent studies, de Barros et al. (2012) and Stark et al. (2013) report a significant increase in the sSFRs observed in LBGs with redshifts. In addition, at  $z < 3$  it has been shown that the AGN fraction is a strong function of the stellar mass of the host galaxy (Xue et al. 2010; Mul-laney et al. 2012, and references therein), ranging from

a few percent at  $\sim 10^9 M_\odot$  to  $>20\%$  at  $>10^{11} M_\odot$ , thus suggesting a low AGN fraction for our sample of LBGs at  $z>6$ . However, while our galaxies, at stellar masses  $\sim 10^9 M_\odot$ , will be amongst the less massive galaxies at  $z<3$ , they are some of the most massive ones at  $z>6$ , as even  $\sim 10^{10} M_\odot$  galaxies are very rare (González et al. 2011). These differences strongly suggest that while the AGN fraction in relatively low- $z$  LBGs is low, the expectation is for a higher fraction in higher redshift LBG populations.

The very low accretion rates estimated in these galaxies is particularly puzzling as the host galaxies are known to have very high specific SFRs (sSFRs) of  $\sim 2\text{--}20 \text{ Gyr}^{-1}$  (González et al. 2010). This means that the galaxies that make up our X-ray stacks are efficiently converting gas to stars, which in turn corresponds to high gas fractions. These galaxies, appear however, unable to fuel growth of a central SMBH. One plausible explanation for our results is that only a small fraction of these drop-out galaxies actually harbor a central BH. But if they do indeed harbor BHs at their centers, why are they not accreting with a significant duty cycle? On the one hand, our results mimic the findings of Laird et al. (2006) X-ray analysis of  $z \sim 3$  LBGs, wherein they report no evidence that LBGs, which are certainly galaxies in which active star formation is occurring, are also preferentially active in nuclear black hole accretion. On the other hand, the non-LBG population at lower redshift ( $z\sim 3$ ), with comparable sSFRs to these higher redshift sources do appear to have high observed AGN fractions, albeit at higher stellar masses, (Mullaney et al. 2012).

The globally averaged star formation rate density as a function of redshift appears to track the accretion rate density onto luminous quasars rather well, and this has led us to believe that star formation and black hole growth occur in tandem, at least from a statistical point of view (Merloni et al. 2004; Zheng et al. 2009). However, this definitely does not imply that this concordance occurs in every galaxy. LBGs might just not be the sites that harbor the most actively growing black holes at  $z>6$ . By selection, our galaxy sample is composed of the most massive galaxies at these redshifts, with stellar masses  $\sim 10^9 M_\odot$ , and are essentially dust-free (e.g., Bouwens et al. 2010; Wilkins et al. 2011). Thus, it is possible that our stack does not contain the population of galaxies whose BHs are actively growing at  $6<z<8$ , if this growth is restricted to dustier and/or less massive galaxies. Such galaxies will be below the detection threshold for even the deepest optical/near-IR surveys carried out by large ground-based telescopes or the HST. This implies either that only relatively small black holes are growing in the early Universe or that it is possible at high redshifts for small galaxies to contain substantial central black holes. This possibility of obese BH galaxies has been recently explored by Agarwal et al. (2013).

This scenario indicates that while it appears that the globally averaged SFR and BH accretion rates track each other in the Universe by and large, these properties are not tightly coupled for all individual sub-samples/sub-populations of galaxies. Hence, co-evolution may not occur for every galaxy at the same time. For instance, in most optically-detected quasars the SMBH accretion rate is typically much higher than  $10^{-3}\times$  the SFR (cf. Fig. 2 in Willott et al. 2013), while X-ray stacking of  $z\sim 2$

star forming galaxies suggests the SMBH accretion rate is at the level  $10^{-3}\times$  the SFR, the scaling needed for co-evolution of the SMBH mass with stellar mass (Mullaney et al. 2012). Clearly the relative timescales of SMBH growth and SFR (Netzer 2009) are a key determinant in the establishment of the correlations between SMBHs and host galaxies, as well as in the interpretation of observational results.

Alternatively, it is also possible that these samples contain a significant fraction of low- $z$  interlopers. The most likely interlopers for high- $z$  galaxy samples include reddened and/or old galaxies at  $z\sim 1\text{--}2$ , low mass stars and spurious or transient sources. All of them have lower X-ray fluxes than average AGN and therefore would artificially decrease the signal in our stacks. The contamination fraction in  $z>6$  galaxy samples have been extensively debated in the past, as shown by example in Appendix D of Bouwens et al. (2006). These results, and others, indicate that typical contamination levels are  $\sim 10\%$  or lower (e.g., Bouwens et al. 2011). If this is indeed the case, the existence of these relatively insignificant fraction of low redshift interlopers cannot significantly change our results or explain the lack of an X-ray detection. However, it is possible that these contamination levels have been significantly underestimated, given that the contribution of more exotic galaxies, such as those with extreme emission lines (Brammer et al. 2013) cannot be properly accounted for.

As proposed by Treister et al. (2011), it is possible that a large fraction of the emission due to accretion onto SMBHs in the early Universe is obscured by large amounts of gas and dust. Our more restrictive constraints here were obtained from the observed-frame soft Chandra band, 0.5-2 keV, which at these high redshifts corresponds to rest-frame energies of  $\sim 2\text{--}10$  keV, i.e., the observed-frame hard Chandra band. Therefore, for these observations to be significantly affected by obscuration would require extremely high levels of obscuration, up to Compton-thick column densities,  $N_H\sim 10^{24} \text{ cm}^{-2}$ . While an increased contribution at high redshift of such heavy obscurations is certainly possible (e.g., Moretti et al. 2012), the observations in the observed-frame hard band trace rest-frame energies of  $\sim 30$  keV, at the peak of the AGN X-ray emission, even for heavily obscured sources. These upper limits, which are roughly  $\sim 10$  times higher than those obtained in the observed-frame soft Chandra band, while would be in marginal agreement with most existing models and expectations, will still generate tension. The lack of any mildly obscured and unobscured AGN at this redshift also raises puzzling questions regarding Unification; though perhaps the explanation lies in the high gas density expected in high-sSFR, compact galaxies - high column densities in all ( $4\pi$ ) directions. Indeed, at lower redshifts Xue et al. (2012) found that most of the low luminosity AGN at similarly low host galaxy stellar masses show evidence for significant obscuration.

Finally, we are implicitly assuming here that black hole growth is due to a radiation-efficient matter accretion (i.e., the Soltan 1982, argument). While this is certainly true in general (e.g., Yu & Tremaine 2002; Marconi et al. 2004), it is possible that is not the case in the early Universe. Specifically, and as argued by Shapiro (2005) and Petri et al. (2012) at  $z>6$  BH growth due to mergers, might dominate over accretion processes. If this is in-

deed the case, BH growth may not be accompanied by luminous emission, or at least not electromagnetic radiation, and thus our X-ray observations are unable to detect it.

### 3.3. Black Hole Masses

The lack of detection of luminous, individually detected, AGN at  $z > 6$  in deep X-ray surveys, together with the upper limits reported here pose interesting and strong limits on the early growth and formation mechanisms for SMBHs. For example, assuming a canonical 10% bolometric correction for hard X-ray emission (e.g., Treister et al. 2009a) and accretion at the Eddington limit implies average BH masses smaller than  $2.7 \times 10^4 M_\odot$  for the  $z \sim 6$  sample (and lower than  $\sim 3 \times 10^5 M_\odot$  for a more typical 10% Eddington ratio), for an AGN fraction of 100% (if a lower AGN fraction is assumed instead, BH masses should be scaled upwards accordingly. For example, they will be smaller than  $\sim 3 \times 10^6 M_\odot$  for a 10% AGN fraction at a 10% Eddington ratio). Furthermore, the luminous quasars detected by optical surveys at  $z > 6$  do contain massive BHs ( $> 10^8 M_\odot$ ) that appear to be accreting near their Eddington limits (Willott et al. 2010a). If the typical galaxy at those redshifts had a smaller BH (scaled down version from the most luminous quasars) growing at similar Eddington ratios or even lower by an order of magnitude, we would have detected them in our study (once the caveats presented in §3.2 are taken into account).

In contrast, many models used to explain the formation and evolution of SMBHs assume large Eddington ratios,  $\gtrsim 30\%$ , thus resulting in relatively massive BHs growing rapidly in the early Universe. For example, the models of Volonteri (2010), in which the accretion is driven by merger-triggered episodes, that tend to bring the resulting BH into the observed  $M$ - $\sigma$  correlation, predict that by  $z \sim 6$  the average masses of the actively-growing BHs should be in the  $\sim 10^6 M_\odot$  range, in marginal agreement with our observations, if relatively low accretion rates and AGN fractions are assumed. A key point to note here about the models is that they hinge on the circular velocity (and therefore halo mass) as the lever for black hole seed masses and the regulation of growth during accretion episodes. In fact, in all current models it is assumed that the accreted mass is proportional to some power of the circular velocity. We caution that it is unclear what the halo masses are for these drop-out galaxies, what we have are only estimates of their average stellar masses. Most BH growth models provide scaling relationships specifically between halo mass and black hole mass and not stellar mass, so direct comparison is complicated by the need to make additional assumptions about the efficiency of star formation in the early Universe.

Given the observed correlation between BH mass and both bulge (Häring & Rix 2004) and total stellar mass (Jahnke et al. 2009) for nearby galaxies, we can estimate the BH mass corresponding to the galaxies in our sample, assuming of course that this correlation holds at high redshifts. Stellar masses were provided for the F12 sample, as derived from spectral fitting. The average stellar mass for the  $z \sim 6$  galaxy sample is  $10^9 M_\odot$  (see also Curtis-Lake et al. 2013), which implies using the Jahnke et al. (2009) relation that typical BH masses are expected

to be  $\sim 10^6 M_\odot$ . This assumes no redshift evolution in the  $M_{BH}$ - $M_*$  relation, consistent with the findings up to  $z \sim 1$  of e.g., Cisternas et al. (2011). Such BH masses are still consistent with the upper limits measured here, provided that both the AGN fraction and the Eddington accretion rates are  $\sim 10\%$  or lower. The growth rate of a BH scales as

$$M(t) = M_0 \times \exp(f_{edd} \times \Delta t \times (1 - \epsilon) / (\epsilon \times 0.45 \text{Gyr})), \quad (4)$$

where  $\Delta t$  is the time allowed for growth, and  $f_{edd}$  is the Eddington ratio,  $\sim 0.1$  in the example above. An AGN fraction of 10% translates into a 10% duty cycle, i.e.,  $\Delta t$  is  $< 10\%$  of the Hubble time at the redshift of interest, of order 1 Gyr at  $z \sim 6$ . Since with these figures the term in the exponent is very small, 0.2 or less, this implies that in this picture BHs do not gain significant mass in the early stages of the Universe.

## 4. CONCLUSIONS

We present here the X-ray properties of samples of  $z \sim 6, 7$  and 8 galaxy candidates in the CDF-S. None of these galaxies are detected in X-ray, either individually or collectively via stacking. This non-detection via the consequent upper limit on the accreted mass density of  $< 1000 M_\odot \text{Mpc}^{-3}$ , offers the most stringent constraints on black hole growth in the early Universe. This is particularly surprising, as our X-ray stacking observations are sensitive enough to detect even moderate amounts of accretion in relatively small black holes. Furthermore, such low accretion levels contradict the predictions of several black hole formation and evolution models and the expectations based on extrapolations of existing AGN luminosity functions.

Explaining these results requires that these high-redshift dropout galaxies, which are now routinely found and studied by HST and large ground-based telescopes, (A) do not contain SMBHs, or (B) if they contain black holes, then these are not growing, or (C) the black hole growth if occurring is heavily obscured and/or not radiating efficiently in X-rays. If BHs are present in these galaxies, we return to the question of why they are not accreting, in particular since they appear to have significant amounts of gas, given their high specific star formation rates. If they do not contain BHs, then our results have new implications for BH seed formation mechanisms; namely, that normal star-forming galaxies at  $6 < z < 8$  are not forming/growing BH seeds at their centers. This may indicate that seed formation and growth in the general galaxy population can be delayed in some cases until much lower redshifts, as suggested by Volonteri & Begelman (2010) and more recently by Bonoli et al. (2012). A particularly remarkable example of such systems was discovered and reported by Schawinski et al. (2011) at  $z = 1.35$ . Our results strongly suggest that the individual sites where the bulk of the stars form at  $6 < z < 8$  may not be the sites that harbor the most massive black holes.

Interestingly many similarities exist between our result and the conclusions drawn by Willott et al. (2010a), based on the comparison between the SMBH and galaxy mass functions at  $z \sim 6$ , that most galaxies at that time formed their stars much more rapidly than their SMBHs grew or that SMBH seeding is inefficient. This conclusion does not of course apply to the most luminous quasars at that epoch, where an increase of the ratio between SMBH



mass and galaxy mass is in fact observed. Therefore, the most massive SMBHs in the most massive galaxies/halos are actively accreting and are on or above the correlation with their hosts (e.g., Wang et al. 2010, and references therein), while at lower galaxy mass either many galaxies do not have SMBHs, or these SMBHs are much less massive than expected, or they are not accreting or obscured. Therefore, there could be significant variations in the strength of the correlation between BH growth and star formation in individual galaxies, or its dependence on galaxy mass (Volonteri & Stark 2011).

We thank the anonymous referee for a careful and thoughtful reading and several useful suggestions, and Dan Coe and Rychard Bouwens for useful discussions on the HUDF data. Support for the work of ET was provided by the Center of Excellence in Astrophysics and Associated Technologies (PFB 06), by the FONDECYT regular grant 1120061 and by the Anillo project ACT1101. KS gratefully acknowledges support from Swiss National Science Foundation Grant PP00P2\_138979/1. PN acknowledges support from the NSF TCAN program via grant AST-1332858.

REFERENCES

Abel, T., Bryan, G. L., & Norman, M. L. 2000, *ApJ*, 540, 39  
 —. 2002, *Science*, 295, 93  
 Agarwal, B., Davis, A. J., Khochfar, S., Natarajan, P., & Dunlop, J. S. 2013, *MNRAS*, 432, 3438  
 Basu-Zych, A. R., Lehmer, B. D., Hornschemeier, A. E., et al. 2013, *ApJ*, 762, 45  
 Begelman, M. C., Volonteri, M., & Rees, M. J. 2006, *MNRAS*, 370, 289  
 Bellovary, J., Brooks, A., Volonteri, M., et al. 2013, arXiv:1307.0856  
 Bonoli, S., Mayer, L., & Callegari, S. 2012, arXiv:1211.3752  
 Booth, C. M. & Schaye, J. 2009, *MNRAS*, 398, 53  
 Bouwens, R. J., Illingworth, G. D., Blakeslee, J. P., & Franx, M. 2006, *ApJ*, 653, 53  
 Bouwens, R. J., Illingworth, G. D., Oesch, P. A., Labbé, I., Trenti, M., van Dokkum, P., Franx, M., Stiavelli, M., Carollo, C. M., Magee, D., & Gonzalez, V. 2011, *ApJ*, 737, 90  
 Bouwens, R. J., Illingworth, G. D., Oesch, P. A., Trenti, M., Stiavelli, M., Carollo, C. M., Franx, M., van Dokkum, P. G., Labbé, I., & Magee, D. 2010, *ApJ*, 708, L69  
 Brammer, G. B., van Dokkum, P. G., Illingworth, G. D., Bouwens, R. J., Labbé, I., Franx, M., Momcheva, I., & Oesch, P. A. 2013, *ApJ*, 765, L2  
 Bromm, V., Coppi, P. S., & Larson, R. B. 2002, *ApJ*, 564, 23  
 Bromm, V. & Loeb, A. 2003, *ApJ*, 596, 34  
 Cisternas, M., Jahnke, K., Bongiorno, A., Inskip, K. J., Impey, C. D., Koekemoer, A. M., Merloni, A., Salvato, M., & Trump, J. R. 2011, *ApJ*, 741, L11  
 Cowie, L. L., Barger, A. J., & Hasinger, G. 2012, *ApJ*, 748, 50  
 Curtis-Lake, E., McLure, R. J., Dunlop, J. S., Schenker, M., Rogers, A. B., Targett, T., Cirasuolo, M., Almaini, O., Ashby, M. L. N., Bradshaw, E. J., Finkelstein, S. L., Dickinson, M., Ellis, R. S., Faber, S. M., Fazio, G. G., Ferguson, H. C., Fontana, A., Grogin, N. A., Hartley, W. G., Kocevski, D. D., Koekemoer, A. M., Lai, K., Robertson, B. E., Vanzella, E., & Willner, S. P. 2013, *MNRAS*, 429, 302  
 de Barros, S., Schaerer, D., & Stark, D. P. 2012, arXiv:1207.3663  
 Dubois, Y., Devriendt, J., Slyz, A., & Teyssier, R. 2012, *MNRAS*, 420, 2662  
 Fan, X., Hennawi, J. F., Richards, G. T., Strauss, M. A., Schneider, D. P., Donley, J. L., Young, J. E., Annis, J., Lin, H., Lampeitl, H., Lupton, R. H., Gunn, J. E., Knapp, G. R., Brandt, W. N., Anderson, S., Bahcall, N. A., Brinkmann, J., Brunner, R. J., Fukugita, M., Szalay, A. S., Szokoly, G. P., & York, D. G. 2004, *AJ*, 128, 515  
 Ferrara, A., Haardt, F., & Salvaterra, R. 2013, *MNRAS*, 434, 2600  
 Fiore, F., Puccetti, S., Grazian, A., et al. 2012, *A&A*, 537, A16  
 Finkelstein, S. L., Papovich, C., Salmon, B., Finlator, K., Dickinson, M., Ferguson, H. C., Gialalisco, M., Koekemoer, A. M., Reddy, N. A., Bassett, R., Conselice, C. J., Dunlop, J. S., Faber, S. M., Grogin, N. A., Hathi, N. P., Kocevski, D. D., Lai, K., Lee, K.-S., McLure, R. J., Mobasher, B., & Newman, J. A. 2012, *ApJ*, 756, 164  
 González, V., Labbé, I., Bouwens, R. J., Illingworth, G., Franx, M., & Kriek, M. 2011, *ApJ*, 735, L34  
 González, V., Labbé, I., Bouwens, R. J., Illingworth, G., Franx, M., Kriek, M., & Brammer, G. B. 2010, *ApJ*, 713, 115  
 Gültekin, K., Richstone, D. O., Gebhardt, K., et al. 2009, *ApJ*, 698, 198  
 Hainline, K. N., Shapley, A. E., Greene, J. E., Steidel, C. C., Reddy, N. A., & Erb, D. K. 2012, *ApJ*, 760, 74  
 Häring, N. & Rix, H.-W. 2004, *ApJ*, 604, L89  
 Hinshaw, G. et al. 2009, *ApJS*, 180, 225  
 Hopkins, P. F., Richards, G. T., & Hernquist, L. 2007, *ApJ*, 654, 731  
 Jahnke, K., Bongiorno, A., Brusa, M., Capak, P., Cappelluti, N., Cisternas, M., Civano, F., Colbert, J., Comastri, A., Elvis, M., Hasinger, G., Ilbert, O., Impey, C., Inskip, K., Koekemoer, A. M., Lilly, S., Maier, C., Merloni, A., Riechers, D., Salvato, M., Schinnerer, E., Scoville, N. Z., Silverman, J., Taniguchi, Y., Trump, J. R., & Yan, L. 2009, *ApJ*, 706, L215  
 Laird, E. S., Nandra, K., Hobbs, A., & Steidel, C. C. 2006, *MNRAS*, 373, 217  
 Lehmer, B. D., Alexander, D. M., Bauer, F. E., Brandt, W. N., Goulding, A. D., Jenkins, L. P., Ptak, A., & Roberts, T. P. 2010, *ApJ*, 724, 559  
 Lodato, G. & Natarajan, P. 2006, *MNRAS*, 371, 1813  
 Loeb, A. & Rasio, F. A. 1994, *ApJ*, 432, 52  
 Madau, P. & Rees, M. J. 2001, *ApJ*, 551, L27  
 Marconi, A., Risaliti, G., Gilli, R., Hunt, L. K., Maiolino, R., & Salvati, M. 2004, *MNRAS*, 351, 169  
 Mayer, L., Kazantzidis, S., Escala, A., & Callegari, S. 2010, *Nature*, 466, 1082  
 Menou, K., Haiman, Z., & Narayanan, V. K. 2001, *ApJ*, 558, 535  
 Merloni, A., Rudnick, G., & Di Matteo, T. 2004, *MNRAS*, 354, L37  
 Mineo, S., Gilfanov, M., & Sunyaev, R. 2012, arXiv:1207.2157  
 Moretti, A., Vattakunnel, S., Tozzi, P., Salvaterra, R., Severgnini, F., Fugazza, D., Haardt, F., & Gilli, R. 2012, *A&A*, 548, A87  
 Mortlock, D. J., Warren, S. J., Venemans, B. P., Patel, M., Hewett, P. C., McMahon, R. G., Simpson, C., Theuns, T., González-Solares, E. A., Adamson, A., Dye, S., Hambly, N. C., Hirst, P., Irwin, M. J., Kuiper, E., Lawrence, A., & Röttgering, H. J. A. 2011, *Nature*, 474, 616  
 Mullaney, J. R., Pannella, M., Daddi, E., Alexander, D. M., Elbaz, D., Hickox, R. C., Bournaud, F., Altieri, B., Aussel, H., Coia, D., Dannerbauer, H., Dasyra, K., Dickinson, M., Hwang, H. S., Kartaltepe, J., Leiton, R., Magdis, G., Magnelli, B., Popesso, P., Valtchanov, I., Bauer, F. E., Brandt, W. N., Del Moro, A., Hanish, D. J., Ivison, R. J., Juneau, S., Luo, B., Lutz, D., Sargent, M. T., Scott, D., & Xue, Y. Q. 2012, *MNRAS*, 419, 95  
 Nandra, K., Mushotzky, R. F., Arnaud, K., Steidel, C. C., Adelberger, K. L., Gardner, J. P., Teplitz, H. I., & Windhorst, R. A. 2002, *ApJ*, 576, 625  
 Natarajan, P. 2011, *Bulletin of the Astronomical Society of India*, 39, 145  
 Netzer, H. 2009, *MNRAS*, 399, 1907  
 Petri, A., Ferrara, A., & Salvaterra, R. 2012, *MNRAS*, 422, 1690  
 Ranalli, P., Comastri, A., & Setti, G. 2003, *A&A*, 399, 39  
 Reddy, N. A., Pettini, M., Steidel, C. C., Shapley, A. E., Erb, D. K., & Law, D. R. 2012, *ApJ*, 754, 25  
 Salvaterra, R., Haardt, F., Volonteri, M., & Moretti, A. 2012, *A&A*, 545, L6  
 Schawinski, K., Urry, M., Treister, E., Simmons, B., Natarajan, P., & Glikman, E. 2011, *ApJ*, 743, L37  
 Shankar, F., Weinberg, D. H., & Miralda-Escudé, J. 2009, *ApJ*, 690, 20  
 Shapiro, S. L. 2005, *ApJ*, 620, 59  
 Silverman, J. D. et al. 2008, *ApJ*, 679, 118  
 Soltan, A. 1982, *MNRAS*, 200, 115  
 Stark, D. P., Schenker, M. A., Ellis, R., Robertson, B., McLure, R., & Dunlop, J. 2013, *ApJ*, 763, 129  
 Szokoly, G. P. et al. 2004, *ApJS*, 155, 271  
 Tan, J. C. & McKee, C. F. 2004, *ApJ*, 603, 383

TABLE 1  
STACKING RESULTS

Redshift	Net counts <sup>a</sup>			Count Rate <sup>b</sup> ( $3\sigma$ ) [s <sup>-1</sup> ]	Flux <sup>b</sup> [erg cm <sup>-2</sup> s <sup>-1</sup> ]	Lum <sup>b</sup> [erg s <sup>-1</sup> ]	BH Mass <sup>b,c</sup> [M <sub>⊙</sub> Mpc <sup>-3</sup> ]	
	B06	B11	F12					
<b>Soft Band (0.5-2 keV)</b>								
$z\sim 6$	-3.4±6.2	—	-3.6±4.7	-4.0±6.5 (272) <sup>d</sup>	<8.9×10 <sup>-8</sup>	<6.5×10 <sup>-19</sup>	<2.6×10 <sup>41</sup>	<851
$z\sim 7$	—	0.7±1.4	-0.6±2.5	-0.4±2.6 (46) <sup>d</sup>	<1.9×10 <sup>-7</sup>	<1.2×10 <sup>-18</sup>	<6.8×10 <sup>41</sup>	<666
$z\sim 8$	—	1.6±1.7	0.7±1.9	1.9±2.1(23) <sup>d</sup>	<3.0×10 <sup>-7</sup>	<2.0×10 <sup>-18</sup>	<1.5×10 <sup>42</sup>	<674
<b>Hard Band (2-8 keV)</b>								
$z\sim 6$	-6.3±9.1	—	-3.3±6.7	-9.1±9.4	<1.7×10 <sup>-7</sup>	<3.4×10 <sup>-18</sup>	<1.6×10 <sup>42</sup>	<4750
$z\sim 7$	—	0.2±2.4	1.8±4.1	1.5±4.1	<3.9×10 <sup>-7</sup>	<7.9×10 <sup>-18</sup>	<5.3×10 <sup>42</sup>	<4704
$z\sim 8$	—	-4.7±2.1	-0.4±2.6	-1.8±2.8	<5.4×10 <sup>-7</sup>	<1.1×10 <sup>-17</sup>	<9.8×10 <sup>42</sup>	<4346

<sup>a</sup>Background subtracted, stacked, counts

<sup>b</sup>For the combined sample

<sup>c</sup>Accreted Black Hole mass density

<sup>d</sup>Number of stacked sources in the combined sample

Treister, E., Schawinski, K., Urry, C. M., & Simmons, B. D. 2012, ApJ, 758, L39  
 Treister, E., Schawinski, K., Volonteri, M., Natarajan, P., & Gawiser, E. 2011, Nature, 474, 356  
 Treister, E., Urry, C. M., & Virani, S. 2009a, ApJ, 696, 110  
 Treister, E. et al. 2009b, ApJ, 706, 535  
 Ueda, Y., Akiyama, M., Ohta, K., & Miyaji, T. 2003, ApJ, 598, 886  
 Verma, A., Lehnert, M. D., Förster Schreiber, N. M., Bremer, M. N., & Douglas, L. 2007, MNRAS, 377, 1024  
 Volonteri, M. 2010, A&A Rev., 18, 279  
 Volonteri, M. & Begelman, M. C. 2010, MNRAS, 409, 1022  
 Volonteri, M. & Stark, D. P. 2011, MNRAS, 417, 2085  
 Wang, R., Carilli, C. L., Neri, R., Riechers, D. A., Wagg, J., Walter, F., Bertoldi, F., Menten, K. M., Omont, A., Cox, P., & Fan, X. 2010, ApJ, 714, 699  
 Wilkins, S. M., Bunker, A. J., Stanway, E., Lorenzoni, S., & Caruana, J. 2011, MNRAS, 417, 717  
 Willott, C. J. 2011, ApJ, 742, L8  
 Willott, C. J., Albert, L., Arzoumanian, D., Bergeron, J., Crampton, D., Delorme, P., Hutchings, J. B., Omont, A., Reylé, C., & Schade, D. 2010a, AJ, 140, 546

Willott, C. J., Delorme, P., Reylé, C., Albert, L., Bergeron, J., Crampton, D., Delfosse, X., Forveille, T., Hutchings, J. B., McLure, R. J., Omont, A., & Schade, D. 2010b, AJ, 139, 906  
 Willott, C. J., Omont, A., & Bergeron, J. 2013, ApJ, 770, 13  
 Xue, Y. Q., Brandt, W. N., Luo, B., et al. 2010, ApJ, 720, 368  
 Xue, Y. Q., Luo, B., Brandt, W. N., Bauer, F. E., Lehmer, B. D., Broos, P. S., Schneider, D. P., Alexander, D. M., Brusa, M., Comastri, A., Fabian, A. C., Gilli, R., Hasinger, G., Hornschemeier, A. E., Koekemoer, A., Liu, T., Mainieri, V., Paolillo, M., Rafferty, D. A., Rosati, P., Shemmer, O., Silverman, J. D., Smail, I., Tozzi, P., & Vignali, C. 2011, ApJS, 195, 10  
 Xue, Y. Q., Wang, S. X., Brandt, W. N., et al. 2012, ApJ, 758, 129  
 Yu, Q. & Tremaine, S. 2002, MNRAS, 335, 965  
 Zheng, X. Z., Bell, E. F., Somerville, R. S., Rix, H.-W., Jahnke, K., Fontanot, F., Rieke, G. H., Schiminovich, D., & Meisenheimer, K. 2009, ApJ, 707, 1566